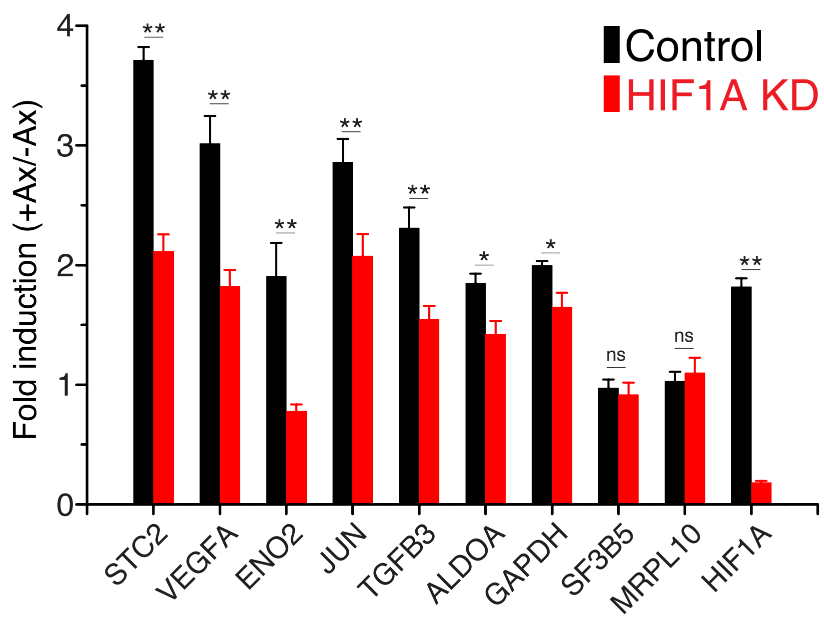

Cho et al., Figure S1 (related to figure 1)

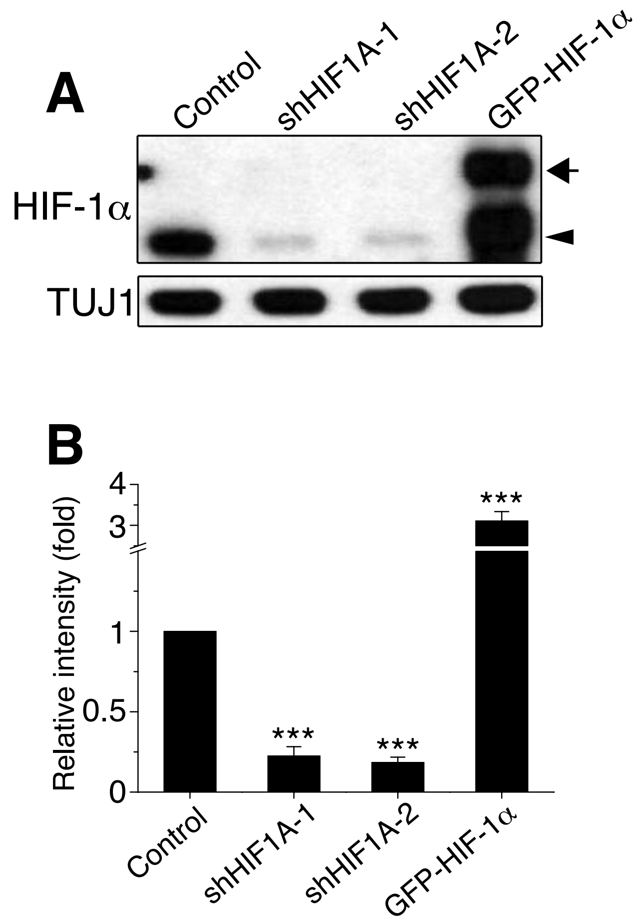

Cho et al., Figure S2 (related to figure 3A)

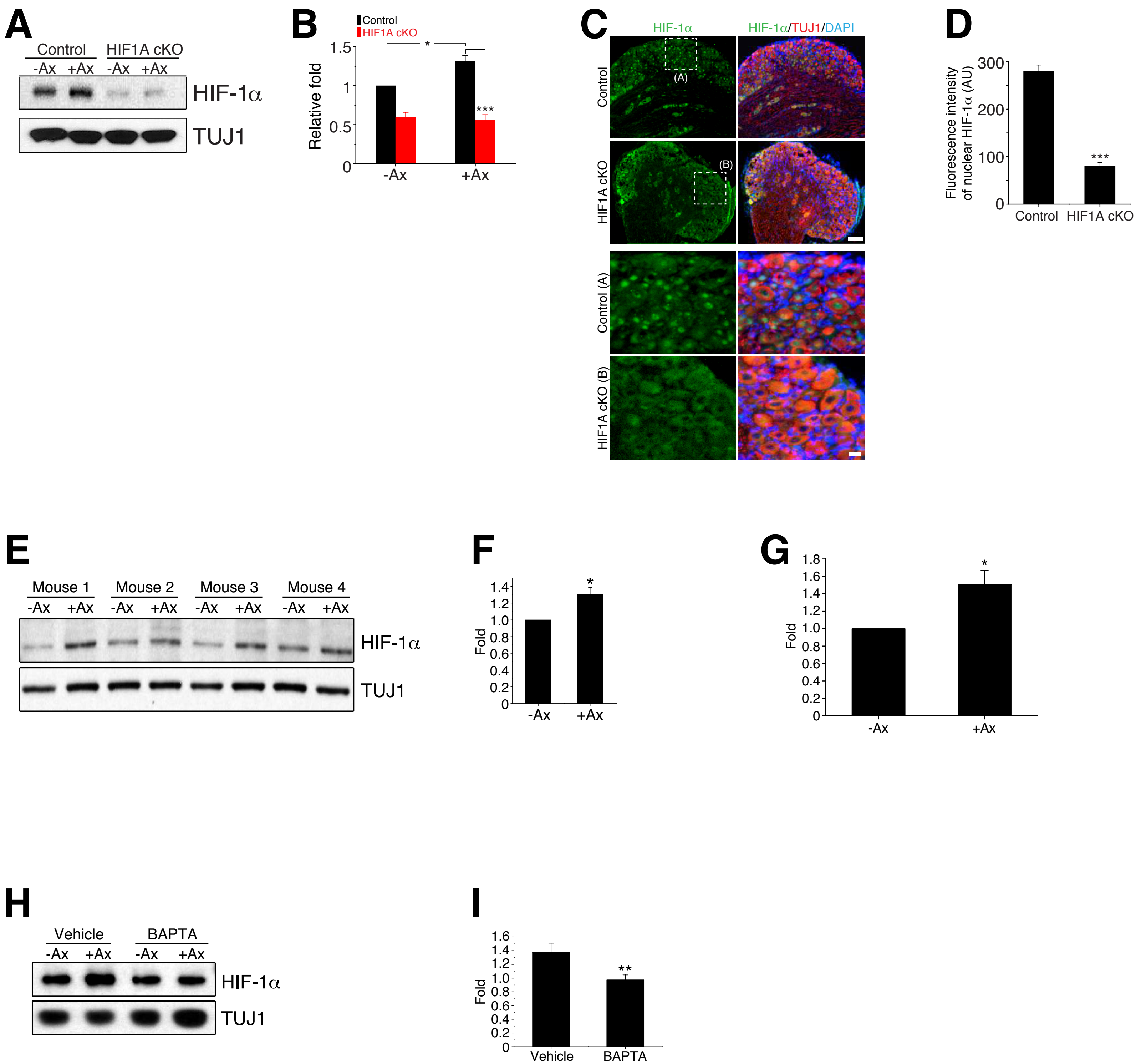

Cho et al., Figure S3 (related to figure 4)

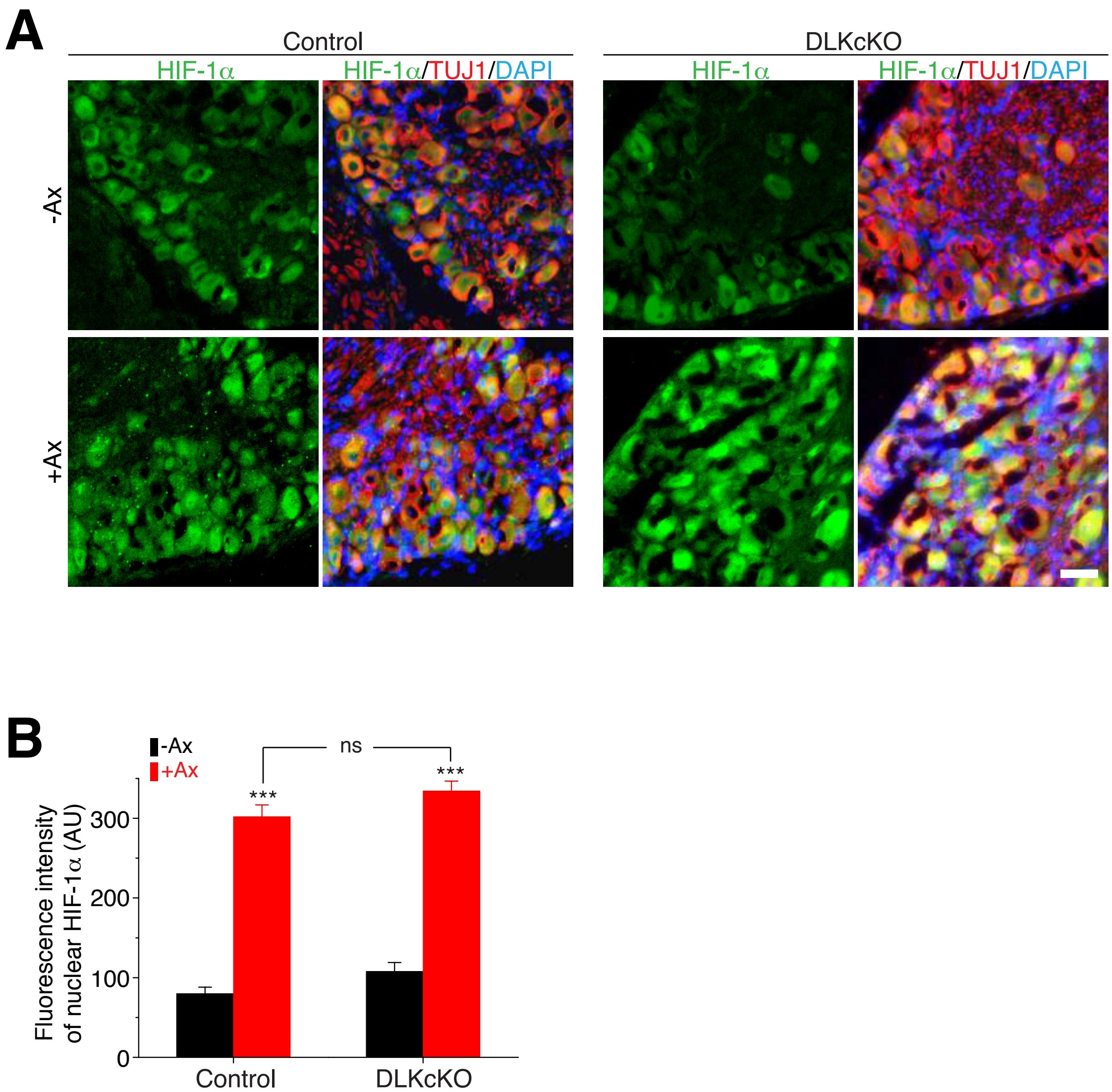

Cho et al., Figure S4 (related to figure 5)

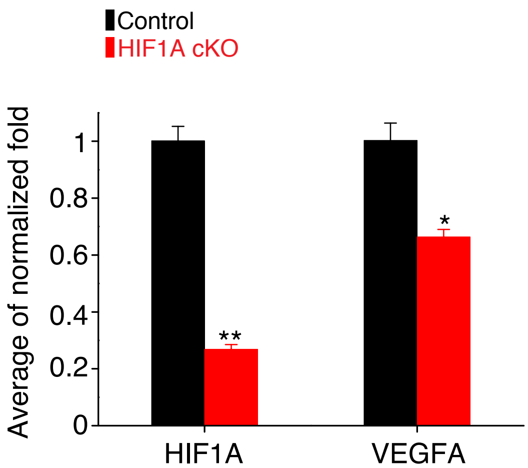

Cho et al., Figure S5 (related to figure 6)

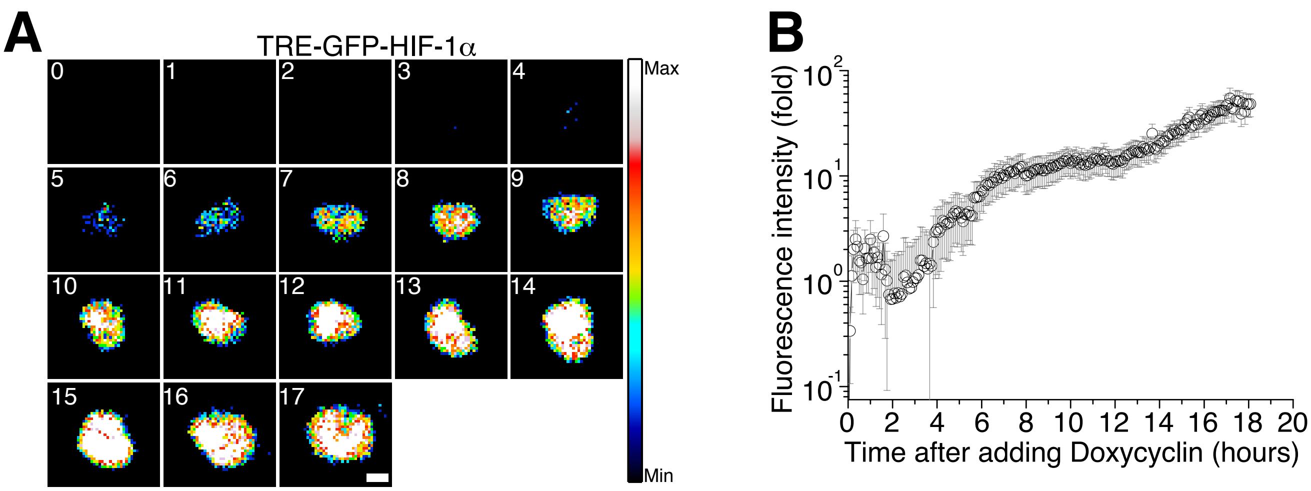

Cho et al., Figure S6 (related to figure 7)

A

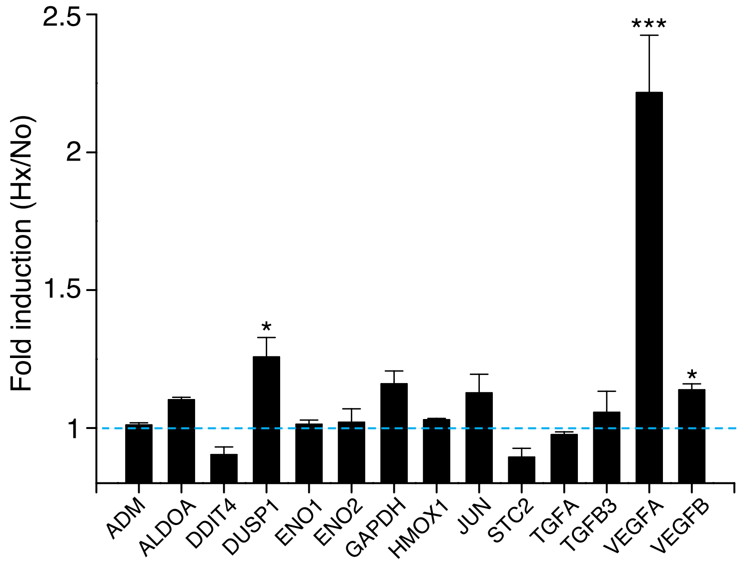

B

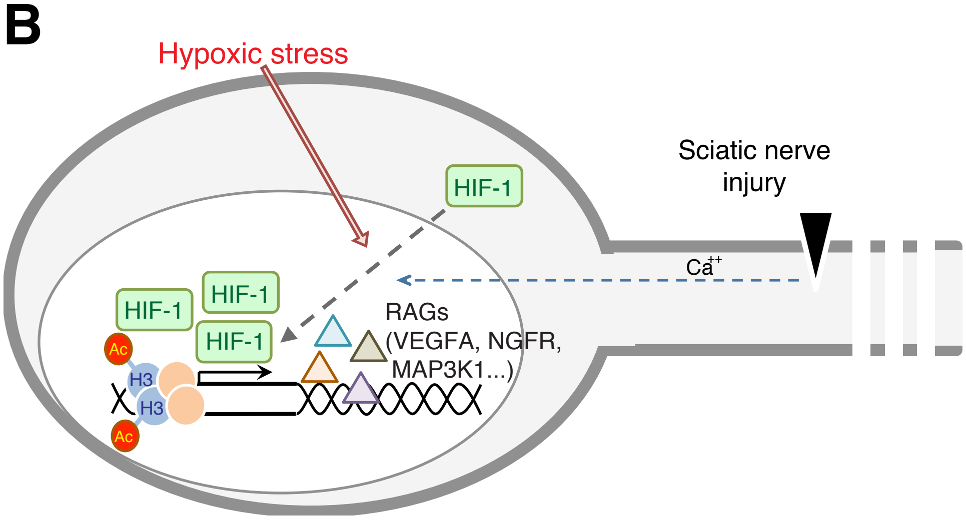

Cho et al., Figure S7 (related to figure 8A)

Supplemental Figure Legends

Figure S1. qPCR analysis of selected HIF-1-target genes. (Related to figure 1).

Quantitative PCR analysis was done using RNA samples prepared from embryonic DRG cultures infected with control or HIF-1α-knock down lentivirus. Seven HIF-1-target genes were tested (STC2, VEGFA, ENO2, JUN, TGFB3, ALDOA and GAPDH). Two genes were used as internal controls to confirm HIF-1-dependency (SF3B5 and MRPL10). Knockdown efficiency of HIF1A was confirmed from the each experimental set (**p<0.01, *p<0.05 by t-test; mean±SEM; ns, not significant).

Figure S2. Knock down or overexpression of HIF-1α in mouse embryonic DRG culture. (Related to figure 3).

(A) HIF-1α was knocked down by two different shRNA lentiviruses (shHIF1A-1 and shHIF1A-2). Human GFP-HIF-1α was overexpressed by lentivirus. Arrowhead points to endogenous HIF-1α and arrow points to GFP- HIF-1α. (B) Normalized intensity calculated from (A) (n=4; ***p<0.001 by one-way ANOVA with Tukey test; mean±SEM)

Figure S3. Expression levels of HIF-1α in control or HIF1AcKO DRGs and following sciatic nerve injury. (Related to figure 4).

(A) Representative western blot of HIF-1α from control or HIF1AcKO mice. L4 and L5 DRGs were dissected from mice that received (+Ax) or not (-Ax) a prior (1 day) sciatic nerve axotomy and analyzed by western blot. (B) HIF-1α were normalized to tubuli (TUJ1) and quantification of

HIF-1α (*n*=3; ***p<0.001, *p<0.05 by one-way ANOVA with Tukey test; mean±SEM). (C) Representative HIF-1α immunostaining from control or HIF1AcKO mice. L4 DRGs were dissected 1 day following sciatic nerve axotomy. Scale bar, 100μm and 20μm (for magnified images (A) and (B)). (D) Quantification of fluorescence intensity of nuclear HIF-1α (*n*=77 and 99 from three control and three HIF1A cKO mice; ***p<0.001 by *t*-test; mean±SEM). (E) Western blot analysis of mouse L4 and L5 DRG tissues dissected at 24 hours after sciatic nerve injury. Protein samples were prepared from four individual mice. (F) Normalized intensity calculated from (A) (*n*=4; *p<0.05 by *t*-test; mean±SEM; -Ax, not injured; +Ax, injured). (G) Expression level of HIF1A mRNA by real time PCR analysis. Mouse L4 and L5 DRG tissues were dissected 24 hours after sciatic nerve injury and prepared for RNA extraction (*n*=4; *p<0.05 by *t*-test, -Ax, not injured; +Ax, injured). (H) Western blot analysis of mouse L4 and L5 DRG tissues dissected 24 hours after sciatic nerve injury in mice that received at the site of injury vehicle or BAPTA-AM treatment. (I) Normalized intensity calculated from (D) (*n*=3; **p<0.01 by *t*-test; mean±SEM; -Ax, not injured; +Ax, injured)

Figure S4. Deletion of DLK in DRG neurons does not alter up-regulation of nuclear HIF-1α induced by sciatic nerve injury. (Related to figure 5).

(A) Immunohistochemistry images of HIF-1α-staining with (+Ax) or without (-Ax) sciatic nerve injury from control or DLKcKO mice. Scale bar, 50μm. Note that in this genetic background, the HIF-1α- staining in the absence of axotomy appears diffuse in the cytoplasm, but nuclear accumulation is clearly induced by injury. (B) Quantification of fluorescence intensity of nuclear HIF-1α (*n*=55, 106, 78 and 89 for control (-Ax), control (+Ax), DLK cKO (-Ax) and DLK cKO (+Ax), respectively. Two mice were used for each condition; ***p<0.001 by one-way ANOVA with Tukey test; mean±SEM; ns, not significant).

Figure S5. Deletion of HIF1A impairs VEGFA gene expression in mouse DRG tissue. (Related to figure 6).

(A) Quantitative PCR analysis of VEGFA from L4 DRGs in control or HIF1A cKO mice (*n*=2 per group, performed in triplicate ; **$p<0.01$, *$p<0.05$ by *t*-test; mean±SEM).

Figure S6. Live imaging showing the nuclear GFP-HIF-1α intensity after Doxycyclin induction. (Related to figure 7).

(A) Representative time-lapse images of GFP-HIF-1α accumulation in the nucleus of cultured DRG neurons. Scale bar, 5μm. The number indicates the hour after Doxycyclin treatment. (B) Average fluorescence intensity calculated from (A) (*n*=6; mean±SEM)

Figure S7. Specific HIF-1-target genes are activated from L4 and L5 DRG tissues after AIH *in vivo*. (Related to figure 8).

(A) Quantitative PCR analysis of fourteen HIF-1-target genes from L4 and L5 DRG tissues after a 2 h AIH regime (*n*=3; ***$p<0.001$, *$p<0.05$ by one-way ANOVA with Tukey test; mean±SEM) . (B). Proposed model for the role HIF-1α in activating a pro-regenerative program. Axon injury induces nuclear accumulation of HIF-1α, possibly via the injury-induced elevation of intracellular calcium ion. Nuclear HIF-1α is required for the injury-induced increase in histone H3 acetylation and for the transcription of injury-responsive genes regulating axon regeneration. Hypoxic stress can be applied after injury, as a post-conditioning, to promote HIF-1α stabilization and improve axon regeneration.

Symbol	PID	3h	8h	12h	40h	3h	8h	12h	40h
AHNAK	PMID: 17437048	3.73	2.04	2.61	1.79	red	red	red	red
ALDOA	PMID: 8955077	0.12	0.14	0.28	0.20	grey	grey	red	grey
ATF4	PMID: 19519398	-0.32	0.27	-0.59	-0.51	black	red	black	black
BBC3	PMID: 17998337	0.97	2.19	1.47	0.23	red	red	red	grey
BCAR1	PMID: 17001309	0.12	0.15	0.27	0.07	grey	grey	red	grey
BHLHB2	PMID: 12354771	-0.14	1.73	0.19	-0.86	black	red	grey	black
BTG1	PMID: 19068236	0.38	1.11	0.74	0.00	red	red	red	black
CCNG2	PMID: 13130303	0.50	0.12	-0.33	0.33	red	grey	black	red
CDKN1B	PMID: 19342889	0.37	0.03	0.72	-0.08	red	grey	red	black
CITED2	PMID: 9887100	0.30	0.10	0.47	0.30	red	grey	red	red
CP	PMID: 10777486	-0.32	-0.16	0.73	0.85	black	black	red	red
CTGF	PMID: 15315937	0.35	-0.46	0.18	0.20	red	black	grey	grey
CTSD	PMID: 13130303	-0.40	0.18	0.36	0.52	black	grey	red	red
CXCL12	PMID: 15235597	1.62	0.26	1.96	1.91	red	red	red	red
CYP2S1	PMID: 17277313	0.18	0.68	0.65	0.69	grey	red	red	red
DDIT4	PMID: 17307335	1.60	1.63	1.26	0.62	red	red	red	red
DUSP1	PMID: 16081065	0.60	1.94	1.33	0.40	red	red	red	red
EGFR	PMID: 16540671	5.16	1.46	5.94	4.21	red	red	red	red
EGLN1	PMID: 14506252	0.81	0.41	0.53	0.20	red	red	red	grey
ETS1	PMID: 11708773	-0.11	-0.30	-0.09	0.45	black	black	black	red
FURIN	PMID: 15611046	-0.29	0.51	0.88	0.00	black	red	red	grey
GPX3	PMID: 15096516	0.35	0.56	0.61	0.96	red	red	red	red
HMOX1	PMID: 13130303	1.64	3.65	2.19	0.10	red	red	red	grey
IGF1R	PMID: 19016246	0.05	-0.38	0.39	0.26	grey	black	red	red
IGFBP3	PMID: 17486380	0.08	0.40	0.06	-0.71	grey	red	grey	black
IRF1	PMID: 11325839	0.11	1.22	0.73	0.19	grey	red	red	grey
ITGB2	PMID: 15235127	-2.74	0.93	1.30	0.73	black	red	red	red
JMY	PMID: 15942958	0.47	1.36	1.17	0.35	red	red	red	red
JUNB	PMID: 16869749	0.42	1.72	1.18	0.04	red	red	red	grey
KRT14	PMID: 13130303	0.40	-0.69	-0.29	-0.48	red	black	black	black
LEP	PMID: 12215445	0.34	0.91	0.85	0.35	red	red	red	red
MAFF	PMID: 16580664	-0.38	1.44	0.95	-1.30	black	red	red	black
MIF	PMID: 16854377	0.26	0.29	0.23	0.33	red	red	grey	red
MMP14	PMID: 15592504	0.11	-0.73	0.13	0.67	grey	black	grey	red
NLK	PMID: 13130303	0.15	-0.08	0.50	-0.07	grey	black	red	black
NOS3	PMID: 12963737	0.22	0.48	0.63	0.88	grey	red	red	red
NRN1	PMID: 16723126	0.06	-0.04	0.02	0.37	grey	black	grey	red
NT5E	PMID: 12370277	-0.86	-2.84	0.00	0.65	black	black	black	red
P4HA2	PMID: 14622280	-0.28	0.61	0.61	0.34	black	red	red	red
PDGFB	PMID: 16136272	-0.57	0.52	0.63	0.04	black	red	red	grey
PFKFB3	PMID: 11744734	-1.22	0.61	-0.20	0.87	black	red	black	red
PFKL	PMID: 13130303	0.32	-0.21	0.19	0.31	red	black	grey	red
PFKP	PMID: 17193925	0.58	-1.38	1.33	0.54	red	black	red	red
PGK1	PMID: 8089148	0.06	0.43	-0.02	0.29	grey	red	black	red
PIM1	PMID: 18708761	-0.31	-0.01	0.10	0.26	black	black	grey	red

Symbol	PID	3h	8h	12h	40h	3h	8h	12h	40h
PLAUR	PMID: 13130303	-1.20	0.76	0.47	0.07	black	red	red	grey
PLOD1	PMID: 14622280	0.47	0.07	0.46	0.41	red	grey	red	red
PLOD2	PMID: 14622280	-0.47	0.57	0.55	0.42	black	red	red	red
PMAIP1	PMID: 14699081	0.92	1.18	0.91	0.62	red	red	red	red
RORA	PMID: 15270719	0.43	2.20	1.34	-0.58	red	red	red	black
SLC2A1	PMID: 15525582	-0.09	0.25	0.37	0.07	black	grey	red	grey
STC2	PMID: 18394600	2.36	2.45	1.15	0.35	red	red	red	red
TEF	PMID: 15073166	0.59	0.28	0.30	1.00	red	red	red	red
TGFA	PMID: 13130303	-0.27	1.87	1.64	0.95	black	red	red	red
TGFB3	PMID: 15155569	0.14	0.41	1.19	1.23	grey	red	red	red
TPI1	PMID: 13130303	0.07	0.15	0.10	0.27	grey	grey	grey	red
VEGFA	PMID: 8756616	0.30	0.72	0.52	-0.17	red	red	red	black
VEGFB	PMID: 11303624	0.10	0.20	0.18	0.37	grey	grey	grey	red
AK3	PMID: 13130303	-0.29	-0.43	-0.45	-0.07	black	black	black	black
COL5A1	PMID: 13130303	-0.07	-0.35	-0.08	-0.20	black	black	black	black
ENO1	PMID: 8955077	0.18	0.02	0.20	0.23	grey	grey	grey	grey
FECH	PMID: 15312748	0.17	0.06	0.18	0.06	grey	grey	grey	grey
HSP90B1	PMID: 15620698	-0.46	-0.52	-0.62	-0.75	black	black	black	black
IGF2	PMID: 13130303	-0.28	-1.12	-0.67	-1.26	black	black	black	black
IGFBP2	PMID: 13130303	0.18	-0.14	-0.04	0.08	grey	black	black	grey
MCL1	PMID: 15611089	-0.50	-0.01	-0.24	-0.27	black	black	black	black
MMP2	PMID: 13130303	0.23	-0.37	0.08	-0.10	grey	black	grey	black
NPM1	PMID: 15310764	-0.18	-0.31	-0.18	-0.14	black	black	black	black
PDGFA	PMID: 15132980	-0.17	0.15	0.05	0.12	black	grey	grey	grey
PDK1	PMID: 16517405	-0.23	-0.12	0.15	0.25	black	black	grey	grey
PPP5C	PMID: 15328343	0.02	0.09	0.13	0.25	grey	grey	grey	grey
TFRC	PMID: 10446187	-0.02	-0.43	-0.21	-0.48	black	black	black	black
TGM2	PMID: 13130303	0.04	-1.75	-0.18	-0.69	grey	black	black	black
VIM	PMID: 13130303	0.07	-0.49	-0.06	-0.29	grey	black	black	black
ADM	PMID: 15155277	-0.91	-0.09	-1.49	-0.90	black	black	black	black
BNIP3	PMID: 10922063	-0.27	-0.22	-0.27	-0.21	black	black	black	black
BNIP3L	PMID: 10922063	-0.27	-0.22	-0.27	-0.21	black	black	black	black
EDN1	PMID: 17554077	-0.11	-1.31	-0.40	-1.75	black	black	black	black
EGLN3	PMID: 15823097	-5.24	0.04	-1.68	-0.83	black	grey	black	black
ERO1L	PMID: 12752442	-0.18	0.15	0.19	0.21	black	grey	grey	grey
GAPDH	PMID: 7929107	0.08	0.09	0.12	0.05	grey	grey	grey	grey
HK1	PMID: 16438736	-0.04	-0.27	0.13	0.19	black	black	grey	grey
ID2	PMID: 15252039	-0.71	-0.45	-1.17	-0.87	black	black	black	black
IGFBP5	PMID: 7684482	-0.22	-0.78	-0.37	-0.97	black	black	black	black
LDHA	PMID: 8955077	-0.02	-0.05	-0.05	0.09	black	black	black	grey
P4HA1	PMID: 14622280	-0.18	-0.36	-0.22	-0.14	black	black	black	black
PDK3	PMID: 18718909	0.05	-0.14	-0.07	-0.09	grey	black	black	black
PGAM1	PMID: 19068236	-0.05	0.05	0.09	0.17	black	grey	grey	grey
PKM2	PMID: 9692838	0.11	0.16	0.12	0.23	grey	grey	grey	grey
TBK1	PMID: 16537515	-0.19	0.10	0.08	0.04	black	grey	grey	grey
TRPC1	PMID: 16709899	-0.10	0.25	0.11	-0.04	black	grey	grey	black

Cho et al., Table S1 (related to figure 1A)

Symbol	3h	8h	12h	40h	3h	8h	12h	40h
ABCB6	0.17	0.05	0.21	0.36	grey	grey	grey	red
ACVR1B	0.36	1.01	0.05	-0.84	red	red	grey	black
AK3L1	-0.14	-0.42	0.54	0.55	black	black	red	red
APLP1	0.27	0.09	0.13	0.35	red	grey	grey	red
AVPI1	0.10	0.46	0.48	0.63	grey	red	red	red
BCKDHA	0.29	0.26	0.39	0.27	red	grey	red	red
BCL2L11	0.23	0.13	2.16	1.92	grey	grey	red	red
BCL6	0.27	-1.04	1.72	0.87	red	black	red	red
BCOR	-0.09	-0.15	0.08	0.34	black	black	grey	red
BMPR2	0.17	0.37	-0.38	0.38	grey	red	black	red
BRSK2	0.33	0.43	0.10	-0.01	red	red	grey	black
CAV1	0.06	-0.65	0.32	-0.31	grey	black	red	black
CCNL1	0.89	-0.09	0.56	0.06	red	black	red	grey
CDH22	-1.36	0.52	-0.08	0.05	black	red	black	grey
DARS	0.28	0.15	-0.03	-0.31	red	grey	black	black
DDR1	0.16	-0.42	0.10	0.55	grey	black	grey	red
DDX4	0.11	0.38	1.06	0.25	grey	red	red	grey
DTNA	0.44	0.30	0.32	-0.03	red	red	red	black
DYSF	-0.98	-0.04	-0.34	0.72	black	black	black	red
ELF3	0.36	1.38	0.64	-0.18	red	red	red	black
FBXO42	0.34	0.48	0.05	0.70	red	red	grey	red
FGF11	0.27	0.16	0.38	0.24	red	grey	red	grey
FIBCD1	0.35	0.50	0.63	1.28	red	red	red	red
FNIP1	-0.01	-0.33	0.68	0.26	black	black	red	grey
GADD45B	0.24	-0.14	1.05	0.58	grey	black	red	red
GJA1	-0.73	-0.68	-0.34	0.33	black	black	black	red
GPT2	0.54	-0.30	-0.11	-0.11	red	black	black	black
GYS1	0.63	0.53	0.37	-0.01	red	red	red	black
HIVEP2	0.20	0.18	-0.29	0.29	grey	grey	black	red
HOMER1	-0.45	0.09	0.70	0.82	black	grey	red	red
HOXA4	0.00	0.19	0.26	0.44	black	grey	grey	red
KLF10	0.70	-1.15	-0.19	0.48	red	black	black	red
KLF4	0.97	1.41	1.26	1.55	red	red	red	red
KLF6	0.02	0.89	-0.20	-0.81	grey	red	black	black
MDGA2	-0.03	0.33	0.39	0.27	black	red	red	red
MNT	-0.40	-0.56	-0.11	0.57	black	black	black	red
MTTP	0.29	0.56	0.31	-0.19	red	red	red	black
NXPH1	0.71	-0.10	-0.44	-1.13	red	black	black	black
OXSR1	-0.31	0.28	-0.22	1.33	black	red	black	red
PIM2	0.42	0.87	0.52	-0.07	red	red	red	black
PLXND1	0.22	0.26	0.60	0.93	grey	red	red	red
PNRC1	0.18	0.29	0.93	0.63	grey	red	red	red
PSD3	-0.03	0.42	0.18	0.07	black	red	grey	grey
RAP2B	-0.19	0.16	0.45	-0.03	black	grey	red	black
RASSF1	0.26	0.07	0.73	0.42	grey	grey	red	red
RCOR2	-0.01	-0.10	0.24	0.32	black	black	grey	red
RORC	0.28	-0.36	-0.40	-4.15	red	black	black	black
SCN1A	-0.14	0.54	0.77	0.07	black	red	red	grey
SFRS5	0.23	0.11	0.18	0.39	grey	grey	grey	red

Symbol	3h	8h	12h	40h	3h	8h	12h	40h
SFXN3	0.13	0.13	0.32	-0.11	grey	grey	red	black
SIAH2	-0.26	-0.54	0.36	-0.18	black	black	red	black
SLC25A36	0.02	-0.08	0.38	0.01	grey	black	red	grey
ST6GAL1	-0.47	-0.07	0.07	0.29	black	black	grey	red
SYT5	0.24	0.17	0.42	0.51	grey	grey	red	red
TCEAL3	0.17	0.33	0.58	0.22	grey	red	red	grey
TEX264	0.24	0.25	0.65	0.46	grey	grey	red	red
TSC22D3	0.73	0.79	0.67	0.38	red	red	red	red
XPNPEP1	0.32	0.25	0.19	-0.26	red	grey	grey	black
YPEL5	0.35	0.62	1.13	1.02	red	red	red	red
ZFX	-0.35	-0.66	1.06	0.62	black	black	red	red
ZNF653	0.28	0.10	-0.01	0.26	red	grey	black	grey
AMOTL2	0.18	-0.12	-0.37	-1.16	grey	black	black	black
ANKRD12	0.11	0.04	-0.04	0.15	grey	grey	black	grey
CHST8	-0.07	-0.26	-0.39	-0.37	black	black	black	black
CLK3	-0.12	0.08	0.00	0.00	black	grey	black	black
EFNA3	-0.21	0.06	0.11	0.12	black	grey	grey	grey
ELOVL4	0.08	0.13	-0.02	0.06	grey	grey	black	grey
EMID2	0.22	0.03	-0.31	-0.53	grey	grey	black	black
GNAI1	0.09	0.07	0.08	-0.10	grey	grey	grey	black
HUWE1	-1.96	-0.71	-1.25	-1.80	black	black	black	black
IER5L	-0.06	0.16	-0.05	0.09	black	grey	black	grey
KLF7	0.15	0.13	-0.01	0.08	grey	grey	black	grey
KLHDC3	0.01	-0.10	-0.06	0.13	grey	black	black	grey
LDB1	0.25	0.16	0.19	0.02	grey	grey	grey	grey
MKNK2	-0.18	-0.08	-0.19	-0.07	black	black	black	black
MTCH2	-0.09	-0.17	-0.46	-0.51	black	black	black	black
NEGR1	-0.91	0.15	-0.41	-2.37	black	grey	black	black
NRXN2	0.02	0.03	0.04	0.15	grey	grey	grey	grey
PCOLCE2	-0.40	-0.46	-0.61	-1.54	black	black	black	black
PCYT1B	-0.46	-0.41	-0.57	-0.21	black	black	black	black
PHF21A	-0.48	-0.06	-0.87	-1.64	black	black	black	black
PLCH2	-0.02	-0.02	-0.13	0.06	black	black	black	grey
PPME1	0.09	0.13	0.11	0.06	grey	grey	grey	grey
PPP1R3C	-0.04	-0.26	0.02	-0.02	black	black	grey	black
PPP1R9A	0.00	0.01	0.00	0.07	grey	grey	grey	grey
PTPRR	-0.16	-0.53	-0.54	-1.14	black	black	black	black
RCOR1	-0.17	0.20	-0.72	-0.82	black	grey	black	black
RRAGD	0.02	-0.09	0.08	-0.17	grey	black	grey	black
SERGEF	-0.04	0.02	0.04	0.05	black	grey	grey	grey
SPOCK1	-0.17	-0.03	-0.11	-0.02	black	black	black	black
TPD52	-0.07	-0.03	-0.27	0.10	black	black	black	grey
UGP2	-0.13	-0.29	-0.22	-0.40	black	black	black	black
UVRAG	0.09	-0.06	-0.10	-0.13	grey	black	black	black
VAPA	-0.61	-0.61	-0.51	-1.01	black	black	black	black
YEATS2	-0.17	0.00	-0.32	0.00	black	black	black	black
ZC3H6	-0.24	-0.03	-0.35	-0.10	black	black	black	black
ZDHHC9	-0.06	-0.04	-0.23	-0.14	black	black	black	black
ZNF292	-0.94	-0.38	-0.64	-0.75	black	black	black	black

Cho et al., Table S2 (related to figure 1B)

PROBE	SYMBOL	Log2[Fold]
ILMN_1213681	0610009O20RIK	1.60
ILMN_2679823	1110059P08RIK	1.57
ILMN_2681984	1300018I05RIK	3.06
ILMN_3008277	1500032D16RIK	0.96
ILMN_2881024	1700040I03RIK	1.07
ILMN_2742293	1810009O10RIK	1.21
ILMN_1246756	1810030N24RIK	1.28
ILMN_1252689	2010106G01RIK	1.69
ILMN_2946608	2310047M10RIK	1.37
ILMN_2950721	2810008M24RIK	0.95
ILMN_2896976	2810030E01RIK	1.32
ILMN_2851455	2810408M09RIK	1.01
ILMN_2964728	2810410C14RIK	2.16
ILMN_2683277	3830406C13RIK	1.10
ILMN_1218703	4930402H24RIK	1.14
ILMN_2693151	4933428G09RIK	1.06
ILMN_2936468	5730596K20RIK	1.51
ILMN_2888375	6230427J02RIK	1.13
ILMN_3161819	6330534C20RIK	1.19
ILMN_2650106	6330578E17RIK	1.12
ILMN_2614853	6720458F09RIK	1.06
ILMN_1232530	8430410K20RIK	1.35
ILMN_2633062	9130422G05RIK	1.08
ILMN_2857095	9630028B13RIK	1.05
ILMN_1213026	9630058J23RIK	1.06
ILMN_2901131	A530088H08RIK	1.08
ILMN_3150233	ABCA3	1.09
ILMN_2768926	ABCF1	1.09
ILMN_2830611	ACCN3	1.01
ILMN_2622671	ACSL1	1.92
ILMN_3143358	ADORA1	1.93
ILMN_2808336	AES	0.99
ILMN_3124160	AMBRA1	1.10
ILMN_2842843	AMPH	1.32
ILMN_2663741	ANKMY2	1.55
ILMN_2675464	ANKRD17	1.93
ILMN_3109098	ANKRD40	1.21
ILMN_1222794	ANKRD46	1.03
ILMN_2595597	ANLN	0.95
ILMN_2669146	AP1GBP1	2.26
ILMN_2762255	AP2S1	1.08
ILMN_2763103	ARF6	1.51
ILMN_3012253	ARMCX6	1.39
ILMN_1225615	ARS2	1.24
ILMN_1225552	ARSA	2.68
ILMN_3154222	ASH2L	2.25
ILMN_1223734	ATF4	1.37
ILMN_3146362	ATMIN	1.43
ILMN_1218058	ATP1A1	1.09
ILMN_2725286	ATP6AP2	1.97
ILMN_3007669	BAT1A	1.24
ILMN_2736975	BAT3	1.40
ILMN_2850073	BC018242	1.42
ILMN_1220980	BC020002	1.82
ILMN_2764549	BC031853	1.72
ILMN_2637733	BC038925	1.43
ILMN_3161878	BID	0.92
ILMN_2763182	BRE	1.35
ILMN_1257078	BTBD1	1.42
ILMN_2856697	CALM2	1.44
ILMN_1228287	CALU	1.55
ILMN_2765196	CAMK2G	1.18
ILMN_1243596	CAMKV	0.99
ILMN_1246107	CASC4	1.07
ILMN_1231762	CASKIN1	1.07
ILMN_1232016	CBX8	1.33
ILMN_2645613	CC2D1A	1.07
ILMN_2716497	CCNE1	2.97
ILMN_2644664	CDC2L6	1.00
ILMN_1250030	CDC42EP1	1.04
ILMN_2728967	CDYL2	0.97
ILMN_2676726	CENPL	1.12
ILMN_2624574	CEP135	1.32
ILMN_2668387	CGGBP1	1.86
ILMN_2985111	CHFR	0.92
ILMN_2723763	CHGA	1.12

PROBE	SYMBOL	Log2[Fold]
ILMN_2681446	CLPB	2.12
ILMN_2620729	COMMD9	1.04
ILMN_2729985	COPS4	1.47
ILMN_2733698	COX7A2	1.40
ILMN_2735735	CSPP1	0.95
ILMN_3110132	D11BWG0517E	2.68
ILMN_1230030	D11WSU47E	1.14
ILMN_2698239	D15ERTD621E	2.23
ILMN_2819530	D15ERTD682E	1.21
ILMN_2842999	D16H22S680E	1.80
ILMN_2596324	D6WSU163E	1.08
ILMN_2691157	DCTN1	1.37
ILMN_2732536	DCTN5	2.55
ILMN_2705849	DECR2	1.33
ILMN_3105499	DLGAP4	1.04
ILMN_2758073	DMTF1	1.26
ILMN_2644621	DNAJB12	1.28
ILMN_2813454	DNAJC15	1.40
ILMN_1230224	DNAJC6	1.78
ILMN_2751925	DPP3	1.07
ILMN_1240571	DPYSL2	2.10
ILMN_2764309	DUSP14	1.27
ILMN_2611295	DUSP26	1.22
ILMN_2765015	EED	1.01
ILMN_2589181	EEF2	1.11
ILMN_3013874	EG434858	1.71
ILMN_2835683	EG667977	1.01
ILMN_2721894	EIF2B4	1.30
ILMN_2956153	EIF4ENIF1	1.06
ILMN_3121717	ELAVL2	0.98
ILMN_2614752	ELOVL6	1.13
ILMN_3158060	EPN2	2.14
ILMN_2957113	ERCC3	1.40
ILMN_2649966	ETFA	1.08
ILMN_2927225	EXDL2	1.34
ILMN_2622041	F8A	1.28
ILMN_2614494	FAH	1.55
ILMN_2668178	FAM109A	0.95
ILMN_1232976	FAM114A2	1.71
ILMN_1221011	FAM164A	1.26
ILMN_3162793	FASTKD1	2.56
ILMN_2876325	FBXO34	1.41
ILMN_2798086	FCHSD2	0.91
ILMN_2643495	FEZ1	0.96
ILMN_2642743	FGF5	1.33
ILMN_2713285	FHL1	1.20
ILMN_2939295	FIS1	1.29
ILMN_2602630	FLAD1	1.28
ILMN_2734683	FSTL1	1.03
ILMN_2650439	GALNT1	1.08
ILMN_2735940	GDAP1	1.15
ILMN_2632206	GNAS	1.20
ILMN_2852217	GNPDA1	0.92
ILMN_1238654	GORASP2	0.95
ILMN_2745005	GPN3	2.76
ILMN_2854983	GPR85	1.19
ILMN_2732092	GRPEL2	1.56
ILMN_2510196	GTPBP1	0.96
ILMN_2759167	GTPBP5	1.32
ILMN_1259559	H1F0	0.97
ILMN_2841280	HABP4	0.93
ILMN_2859254	HAGHL	1.27
ILMN_1244324	HDGF	1.17
ILMN_3025192	HEL308	1.02
ILMN_2511051	HNRPC	0.98
ILMN_2662054	HPCAL4	2.16
ILMN_2800687	HR	1.54
ILMN_2756369	HSBP1	1.48
ILMN_1228557	ID2	2.61
ILMN_1228213	IFI30	2.40
ILMN_1245193	KCNK10	1.70
ILMN_2590488	KHDRBS3	1.40
ILMN_1216662	KIF5C	2.52
ILMN_2751988	KITL	1.50
ILMN_2592779	KLHL9	1.00
ILMN_1250856	KPNA1	0.93

PROBE	SYMBOL	Log2[Fold]
ILMN_2773211	KRAS	1.36
ILMN_2876712	KRBA1	0.97
ILMN_2999167	L2HGDH	2.58
ILMN_2755152	LETM1	1.03
ILMN_2793616	LIN54	0.97
ILMN_1252919	LMAN2	1.08
ILMN_1255629	LOC100040919	0.92
ILMN_1239024	LOC100044468	1.33
ILMN_2710312	LOC100046650	1.12
ILMN_2445324	LOC100047651	1.71
ILMN_2704855	LOC100047674	0.99
ILMN_2697918	LOC381302	1.16
ILMN_3160792	LOC666676	1.25
ILMN_3111744	LPIN1	0.95
ILMN_2684397	LRRC24	1.01
ILMN_1239448	MANBAL	1.12
ILMN_2598692	MARK3	1.14
ILMN_2978838	MAT2A	1.11
ILMN_2743902	MATK	1.02
ILMN_3111298	MCFD2	1.44
ILMN_2468617	MED12	1.47
ILMN_2669774	METTL8	1.99
ILMN_2971204	MLH3	1.32
ILMN_2678431	MNS1	2.33
ILMN_2685811	MPDU1	1.01
ILMN_2812244	MPPE1	1.46
ILMN_1225936	MRPS30	0.97
ILMN_1226275	MTRF1L	1.26
ILMN_2647873	NAV1	2.74
ILMN_2722864	NCAM1	1.08
ILMN_2619380	NCKIPSD	1.16
ILMN_2693976	NCL	0.92
ILMN_2599997	NCOR1	1.28
ILMN_2914418	NCSTN	1.22
ILMN_2900025	NDUFS4	1.42
ILMN_2657467	NELF	1.41
ILMN_3151722	NET1	0.92
ILMN_2991107	NHEJ1	1.34
ILMN_2778195	NIN	1.15
ILMN_1226280	NOLA1	3.01
ILMN_1247930	NQO2	1.26
ILMN_3014084	NR1H2	1.00
ILMN_2888742	NTAN1	1.81
ILMN_2615312	NTN2L	1.02
ILMN_2750402	NUDT19	1.02
ILMN_2644140	PANK4	0.98
ILMN_1214488	PEBP1	1.58
ILMN_2766262	PFDN5	1.37
ILMN_1253966	PFKFB2	1.05
ILMN_2846254	PGPEP1	1.04
ILMN_2669782	PHCA	1.07
ILMN_2780759	PKNOX1	2.11
ILMN_2731769	PLEKHB2	0.91
ILMN_2749448	PLEKHO2	1.39
ILMN_2791272	POR	1.33
ILMN_2884610	PPAPDC1B	1.07
ILMN_2760691	PPP2R2C	1.57
ILMN_2953411	PPP3R1	1.18
ILMN_2688607	PPTC7	0.97
ILMN_2732229	PRDX3	1.22
ILMN_2833378	PRKACA	1.18
ILMN_1237939	PRKRIR	0.95
ILMN_1243722	PROSAPIP1	1.26
ILMN_2793488	PSMA7	1.93
ILMN_2986309	PSME1	1.08
ILMN_1239565	PTPRT	1.80
ILMN_3082864	PVRL3	1.45
ILMN_1228613	PYCRL	0.93
ILMN_2588572	RAB14	1.53
ILMN_1250569	RAPGEFL1	1.06
ILMN_2699663	RASGRF1	1.11
ILMN_3104139	RBM12	1.09
ILMN_3163340	RBM45	1.01
ILMN_2685477	RDH14	1.35
ILMN_3043469	RET	1.01
ILMN_2974460	RHOBTB2	1.64

PROBE	SYMBOL	Log2[Fold]
ILMN_1216534	RIC3	1.22
ILMN_1237399	RIT2	0.96
ILMN_2637639	RPS3	0.99
ILMN_1223145	RQCD1	1.15
ILMN_2724545	SBK	1.97
ILMN_2759669	SCAF1	1.06
ILMN_1239210	SCN11A	1.43
ILMN_2635631	SEMA3F	0.99
ILMN_1226447	SEMA4B	0.92
ILMN_2776377	SFXN4	1.69
ILMN_1255256	SGCB	1.39
ILMN_3139354	SH2B1	0.93
ILMN_2636212	SH3BGRL	0.95
ILMN_2592285	SKP2	0.94
ILMN_3146420	SLC12A2	2.68
ILMN_2600053	SLC25A11	1.70
ILMN_2886162	SLC45A4	2.63
ILMN_1257987	SLC7A3	0.91
ILMN_3120652	SMAP2	2.59
ILMN_3154810	SMARCA2	1.52
ILMN_1248397	SMARCD3	1.23
ILMN_2705578	SNX30	1.29
ILMN_2710705	SQSTM1	1.26
ILMN_2600537	SRI	1.16
ILMN_2693461	SSBP2	0.98
ILMN_1225487	ST8SIA1	1.18
ILMN_3155190	STK35	1.72
ILMN_1220815	SYT5	3.18
ILMN_2668020	SYT9	0.96
ILMN_3009839	TADA2L	1.76
ILMN_2650732	TAF15	1.32
ILMN_2711782	TBC1D1	1.21
ILMN_2907473	TBC1D10A	1.09
ILMN_2995698	TCEB1	1.13
ILMN_3112736	TCF25	1.70
ILMN_2650683	TDRD3	0.94
ILMN_2961626	THEM2	1.33
ILMN_3141249	THSD4	1.34
ILMN_2589211	TIMM44	1.05
ILMN_3002943	TMED10	1.16
ILMN_2640348	TMEM110	1.12
ILMN_2859294	TMEM111	1.08
ILMN_2643021	TMEM169	0.93
ILMN_1244836	TMEM41A	1.26
ILMN_2881296	TMEM66	1.16
ILMN_1238661	TRAPPC3	1.26
ILMN_2837779	TRPV2	1.39
ILMN_2654568	TRUB1	1.72
ILMN_2638061	TSC22D4	1.21
ILMN_2622057	TSEN2	1.55
ILMN_3083981	TTC5	1.13
ILMN_2949605	UBAC2	1.00
ILMN_2746776	UBP1	0.93
ILMN_2970879	UCHL3	1.28
ILMN_1242013	UCK2	1.20
ILMN_1244059	ULK2	1.48
ILMN_1245461	USP52	0.97
ILMN_2485148	VAPA	1.36
ILMN_2506144	VAPB	1.24
ILMN_2631192	VPS26B	2.05
ILMN_2826414	WDFY3	1.96
ILMN_1242852	WDR45L	2.58
ILMN_2426921	WDR5	1.97
ILMN_2680852	WDR59	2.06
ILMN_2682516	WIPI2	1.19
ILMN_1230273	XPC	1.59
ILMN_2595026	YOD1	1.36
ILMN_2966722	YWHAH	1.36
ILMN_2507227	ZC3H3	1.60
ILMN_2951955	ZCCHC3	1.03
ILMN_2791551	ZCRB1	0.94
ILMN_1214224	ZFP1	1.65
ILMN_2508745	ZFYVE21	1.28
ILMN_2424555	ZKSCAN6	1.14
ILMN_2497067	ZMYND11	1.63
ILMN_2971486	ZNRD1	2.00

PROBE	SYMBOL	Log2[Fold]
ILMN_3100456	1110002B05RIK	-1.62
ILMN_1229545	1110007M04RIK	-1.72
ILMN_1251160	1110036O03RIK	-1.69
ILMN_2795412	1190002A17RIK	-2.43
ILMN_2677494	1700025G04RIK	-2.17
ILMN_1242802	1810026J23RIK	-1.99
ILMN_1229238	2010005J08RIK	-1.69
ILMN_1232589	2010321M09RIK	-2.34
ILMN_2986899	2210418O10RIK	-1.54
ILMN_1238640	2310003H01RIK	-3.84
ILMN_2614728	2310008H09RIK	-1.55
ILMN_2597032	2310036D22RIK	-1.87
ILMN_2899022	2510012J08RIK	-1.99
ILMN_2910230	2610510J17RIK	-1.63
ILMN_2690410	2610528E23RIK	-2.09
ILMN_2724868	4732496O08RIK	-1.93
ILMN_2590975	4930455F23RIK	-1.54
ILMN_1259754	4930572J05RIK	-2.76
ILMN_2668114	4933421E11RIK	-2.28
ILMN_1220446	4933439C20RIK	-2.19
ILMN_2741790	5730449L18RIK	-2.87
ILMN_2888842	5730589K01RIK	-1.86
ILMN_2608043	6330503C03RIK	-1.97
ILMN_2681516	6330503K22RIK	-1.60
ILMN_2624280	6430706D22RIK	-1.68
ILMN_2725428	6620401K05RIK	-1.62
ILMN_2647627	6720456B07RIK	-2.60
ILMN_2702989	9030425E11RIK	-1.60
ILMN_1217864	9430015G10RIK	-1.55
ILMN_2705227	9630015D15RIK	-1.82
ILMN_2605400	A030010B05RIK	-1.63
ILMN_2517060	A930025D01RIK	-3.67
ILMN_3072957	AAMP	-1.55
ILMN_1220310	ABHD7	-2.00
ILMN_2687723	ACADM	-1.63
ILMN_2612683	ACADSB	-2.93
ILMN_2671176	ACBD3	-2.56
ILMN_1237750	ACTB	-1.56
ILMN_2740222	ACY1	-2.33
ILMN_2903734	ADK	-1.72
ILMN_2945472	ADNP	-4.41
ILMN_2675261	ADPGK	-1.55
ILMN_3143483	ADRM1	-1.77
ILMN_2594821	AGGF1	-2.69
ILMN_3134078	AGPAT3	-1.67
ILMN_2643832	AGPS	-1.60
ILMN_2934120	AK2	-1.74
ILMN_2801380	ANK2	-2.26
ILMN_2859518	ANKRD54	-1.63
ILMN_1249598	ANKS1	-2.03
ILMN_2592925	ANKS3	-2.53
ILMN_2948649	ANKZF1	-2.20
ILMN_2760088	ANO10	-1.94
ILMN_2935734	AP1GBP1	-2.35
ILMN_1223335	AP3B1	-3.87
ILMN_2856668	APPBP2	-2.35
ILMN_2588055	ARHGAP29	-1.71
ILMN_1242419	ARMCX5	-1.94
ILMN_2872599	ARPC5	-2.53
ILMN_1250857	ASCC1	-2.47
ILMN_2473348	ASNS	-1.84
ILMN_1254736	ATG5	-1.61
ILMN_3006123	ATIC	-4.75
ILMN_2759598	ATOX1	-1.54
ILMN_1244460	ATP13A2	-1.56
ILMN_1235962	ATP6V1D	-2.22
ILMN_2893992	ATPAF2	-1.58
ILMN_2984999	AVIL	-1.86
ILMN_2702704	B020018G12RIK	-1.93
ILMN_2666155	B230312A22RIK	-2.46
ILMN_2837156	B4GALT1	-2.16
ILMN_2712873	BC018242	-1.99
ILMN_2667369	BC022224	-3.61
ILMN_2785605	BC038156	-1.69
ILMN_2832620	BCKDK	-2.01
ILMN_1252682	BCL2L2	-1.54
ILMN_2959285	BCORL1	-1.91
ILMN_2789562	BIN1	-2.25
ILMN_2668243	BRCC3	-2.63
ILMN_2795040	BXDC5	-1.55
ILMN_2491654	C430003P19RIK	-1.79
ILMN_1213929	CACNA1B	-4.18
ILMN_1216985	CARKD	-1.65
ILMN_2747820	CCDC109A	-1.98
ILMN_2835012	CCDC126	-1.85
ILMN_1258028	CCDC21	-1.57
ILMN_2788154	CCDC88A	-1.93
ILMN_2701355	CD164	-2.05
ILMN_2721724	CD248	-2.37
ILMN_2845312	CDC25A	-2.07
ILMN_2883561	CDK9	-1.90
ILMN_2692306	CETN4	-1.53
ILMN_2746830	CFP	-2.01
ILMN_2867013	CHCHD4	-2.10
ILMN_1246611	CHMP5	-2.06
ILMN_1218263	CHRM3	-1.58
ILMN_2601020	CIC	-2.77
ILMN_1240318	CKLF	-2.10
ILMN_2940227	CLK2	-2.20
ILMN_2716838	CLPP	-2.36
ILMN_1215810	CNOT10	-1.75
ILMN_2669128	CNOT3	-2.80
ILMN_1227218	CNOT4	-2.78
ILMN_2482026	COG6	-2.98
ILMN_2616461	COMMD6	-2.13
ILMN_2731424	COPS2	-1.53
ILMN_2936517	COPZ2	-2.23

PROBE	SYMBOL	Log2[Fold]
ILMN_2869623	COX6A1	-1.59
ILMN_1235500	CRTAP	-2.65
ILMN_2767187	CRYZ	-1.65
ILMN_2598775	CSDE1	-1.63
ILMN_2945483	CTNNBIP1	-1.60
ILMN_2634338	CUL4A	-1.61
ILMN_2954195	CYB5R3	-1.86
ILMN_3001013	CYLD	-2.47
ILMN_2636832	D15WSU169E	-3.50
ILMN_3148398	D5ERTD579E	-2.00
ILMN_2737163	D930036B08RIK	-2.03
ILMN_2700765	D9ERTD392E	-3.34
ILMN_2667101	DAB2IP	-1.74
ILMN_2873510	DAPK3	-2.46
ILMN_2859032	DBR1	-1.59
ILMN_2773485	DCTD	-1.65
ILMN_1236131	DCTN4	-1.85
ILMN_2811861	DCUN1D4	-1.87
ILMN_1237651	DDX20	-2.30
ILMN_2630293	DDX49	-3.70
ILMN_3051392	DENND5A	-1.62
ILMN_2946901	DENR	-1.66
ILMN_2840327	DHRS7	-2.40
ILMN_1241225	DNAJB1	-2.27
ILMN_1225520	DNAJB2	-1.53
ILMN_1254562	DPP9	-1.57
ILMN_3102035	DRG2	-3.27
ILMN_2603662	DUS1L	-1.99
ILMN_1240323	DXBWG1396E	-5.03
ILMN_2897468	EARS2	-1.62
ILMN_2749303	EBNA1BP2	-2.40
ILMN_2944601	EFNA1	-2.18
ILMN_2800655	EFNA3	-1.89
ILMN_1222806	EG433182	-1.79
ILMN_3020829	ELAVL4	-2.87
ILMN_3108203	ELP2	-2.51
ILMN_1227277	EPRS	-1.58
ILMN_2732576	ERCC5	-1.81
ILMN_2502623	ETFA	-1.89
ILMN_2985305	EXOSC10	-3.34
ILMN_2601590	FARSB	-1.66
ILMN_2683933	FASTK	-2.01
ILMN_2724595	FBXL4	-2.08
ILMN_2796353	FBXO7	-1.90
ILMN_1253844	FEM1C	-1.94
ILMN_2432550	FGF13	-3.17
ILMN_3159730	FKBPL	-1.62
ILMN_2701365	FLOT1	-1.54
ILMN_1244077	FNTA	-2.93
ILMN_2914510	GAL3ST1	-2.82
ILMN_2702508	GAPDH	-2.51
ILMN_2753687	GFOD1	-2.52
ILMN_1234981	GLG1	-1.62
ILMN_2788574	GM1943	-1.96
ILMN_2657694	GM3258	-1.58
ILMN_2647048	GM9731	-1.85
ILMN_2958417	GMIP	-1.59
ILMN_2730701	GOPC	-1.78
ILMN_2741629	GPR153	-1.60
ILMN_2972149	GPR162	-1.58
ILMN_2734060	GPR22	-1.71
ILMN_2779636	GPRK6	-1.97
ILMN_2472861	GRIPAP1	-1.61
ILMN_2996732	GRIT	-1.55
ILMN_2792809	GSTK1	-1.81
ILMN_2660438	GTDC1	-1.96
ILMN_2847618	GTF2E2	-1.67
ILMN_1256420	HADHB	-1.90
ILMN_1225037	HBB-Y	-4.12
ILMN_2792924	HCFC2	-4.22
ILMN_2788065	HEATR5A	-1.59
ILMN_1241618	HELZ	-1.61
ILMN_3123341	HES6	-2.12
ILMN_1232121	HINT2	-1.54
ILMN_2895862	HIP2	-3.36
ILMN_1225014	HIST1H2AD	-2.59
ILMN_2733514	HIST1H4K	-2.20
ILMN_2654314	HIST2H3B	-1.98
ILMN_3070951	HNRNPK	-1.55
ILMN_3143304	HNRPA1	-2.73
ILMN_2533766	HOOK2	-1.56
ILMN_2610309	HOXA4	-2.14
ILMN_1254113	HOXD4	-1.76
ILMN_1224336	HSPA4	-1.90
ILMN_3105936	HYOU1	-2.10
ILMN_3132262	IFNA6	-2.23
ILMN_2729235	IFT20	-1.92
ILMN_2637365	IGF2BP2	-1.71
ILMN_2506115	IHPK2	-2.36
ILMN_2661367	IMPACT	-3.82
ILMN_2453620	INO80C	-2.07
ILMN_1218266	IPP	-1.68
ILMN_1235785	ISCA1	-1.65
ILMN_2760514	JAKMIP1	-2.25
ILMN_2755860	KCNK4	-1.91
ILMN_2940017	KIF1B	-1.60
ILMN_3124226	KIN	-2.30
ILMN_1214486	KRTCAP3	-1.87
ILMN_2636435	KTELC1	-1.58
ILMN_2627350	LASS2	-2.20
ILMN_2933993	LAT2	-1.99
ILMN_2703321	LBH	-2.35
ILMN_2615559	LEPROTL1	-1.65
ILMN_2660898	LGI1	-1.59
ILMN_2740523	LOC100043257	-1.59
ILMN_2456617	LOC100044177	-1.78
ILMN_1377924	LOC100046039	-1.81

PROBE	SYMBOL	Log2[Fold]
ILMN_1232447	LOC100047009	-1.95
ILMN_2744204	LOC100047837	-1.79
ILMN_2611874	LOC675228	-2.53
ILMN_2745480	LRRC45	-2.49
ILMN_1218264	MAGOH	-2.21
ILMN_2669982	MANBA	-2.16
ILMN_2657822	MAP3K14	-1.70
ILMN_2757716	MAP4K2	-1.68
ILMN_2924969	MAPK6	-1.59
ILMN_1235783	MAPK8	-2.30
ILMN_1232762	MARCH7	-2.21
ILMN_1230454	MARK3	-2.12
ILMN_2665050	MAST1	-3.93
ILMN_2670352	MAT2A	-2.76
ILMN_2860196	MCM2	-3.08
ILMN_2451377	MCTS1	-1.79
ILMN_2453695	MECR	-2.05
ILMN_1235000	MED22	-1.68
ILMN_2590894	MED28	-2.43
ILMN_2994895	MEIS1	-1.58
ILMN_1231396	METAP2	-1.80
ILMN_1248892	METT11D1	-1.76
ILMN_2739599	MEX3A	-2.08
ILMN_2963754	MGLL	-1.62
ILMN_2837543	MIR16	-1.73
ILMN_2986315	MMP24	-1.69
ILMN_2647028	MOBKL3	-2.65
ILMN_3149944	MPPED1	-2.35
ILMN_1258415	MRE11A	-1.56
ILMN_1234453	MRGPRA2	-2.53
ILMN_1220362	MRPL34	-1.71
ILMN_2770585	MRPL48	-1.70
ILMN_1216970	MRPL53	-2.19
ILMN_1246694	MRPS25	-1.87
ILMN_1232495	MTCH2	-2.48
ILMN_2664950	MTRF1	-2.07
ILMN_2704110	MTVR2	-1.80
ILMN_1231096	MTX1	-1.86
ILMN_2492161	MYG1	-1.65
ILMN_1222760	MYO18A	-2.06
ILMN_2610861	MYO5A	-1.70
ILMN_2840985	N6AMT1	-1.84
ILMN_2933426	NACC2	-2.52
ILMN_2654186	NAGK	-1.59
ILMN_1258782	NANOS1	-2.69
ILMN_1222917	NCOA6	-1.65
ILMN_2877541	NDUFA12	-1.62
ILMN_3107273	NDUFA9	-1.97
ILMN_2642546	NDUFAF1	-1.97
ILMN_2805207	NDUFB2	-2.13
ILMN_1246044	NDUFC1	-2.05
ILMN_2719460	NDUFV1	-1.75
ILMN_1238520	NEDD9	-1.72
ILMN_2665889	NOSIP	-1.59
ILMN_2461345	NPM3	-2.03
ILMN_2692942	NR6A1	-1.59
ILMN_2896843	NRAS	-1.88
ILMN_2884646	NRXN1	-1.93
ILMN_2754015	NSUN5	-1.59
ILMN_2621588	NT5C2	-3.67
ILMN_1228797	NUP62	-2.91
ILMN_2723826	OBFC2B	-2.09
ILMN_2805261	OCIAD1	-1.75
ILMN_2740419	OCRL	-1.78
ILMN_2604056	OG9X	-4.10
ILMN_2833985	ORC5L	-1.60
ILMN_2991930	P4HA2	-2.66
ILMN_1226157	PABPC4	-2.17
ILMN_1254380	PARL	-1.87
ILMN_2509918	PCDHA6	-2.95
ILMN_1251876	PCOLCE2	-1.94
ILMN_1257244	PEMT	-1.95
ILMN_3082287	PEX19	-2.26
ILMN_3076948	PHC1	-1.63
ILMN_2625060	PHF2	-1.94
ILMN_2605096	PIK3R3	-1.65
ILMN_2974480	PML	-1.53
ILMN_1214991	POFUT1	-1.59
ILMN_1239087	POLR2F	-5.80
ILMN_2773464	POR	-3.95
ILMN_2984462	PPM1B	-2.08
ILMN_2776910	PPM1G	-2.18
ILMN_2683620	PPM1L	-1.83
ILMN_3132204	PPP1CB	-3.74
ILMN_2690460	PPP4R1	-1.57
ILMN_3153982	PQLC3	-1.96
ILMN_1243654	PREB	-2.13
ILMN_2746107	PSMB6	-1.61
ILMN_2624695	PTGR2	-1.56
ILMN_2720930	PTPLAD1	-2.61
ILMN_2956895	PTPN1	-2.47
ILMN_1250907	PTPRE	-1.79
ILMN_1232182	PYROXD1	-1.85
ILMN_2435079	RAB6	-3.46
ILMN_1252302	RAD23B	-2.01
ILMN_2810473	RAD9	-2.53
ILMN_1228426	RAGE	-1.67
ILMN_1218612	RER1	-1.80
ILMN_1226540	RFX1	-1.71
ILMN_2974280	RILPL2	-1.99
ILMN_1249301	RNF138	-1.90
ILMN_2588832	RNF4	-1.99
ILMN_2818879	RP9	-1.80
ILMN_3163029	RPS13	-1.67
ILMN_1248304	RPS24	-2.02
ILMN_2749847	RPS27L	-1.61
ILMN_1216854	RSL1D1	-2.01

PROBE	SYMBOL	Log2[Fold]
ILMN_1213030	RSPO2	-2.76
ILMN_2984935	RUFY2	-3.91
ILMN_1249719	RUVBL2	-1.60
ILMN_2659132	SCYL1	-1.95
ILMN_2609809	SEC61B	-1.69
ILMN_1259737	SEPT2	-1.65
ILMN_2864393	SERTAD3	-1.64
ILMN_1258136	SEZ6L2	-2.36
ILMN_3096701	SF3B4	-2.10
ILMN_1229975	SH3GL1	-1.87
ILMN_1219807	SH3RF1	-1.70
ILMN_2948971	SIAH1B	-2.83
ILMN_1258677	SIL1	-1.81
ILMN_1245987	SIRT6	-1.89
ILMN_1235909	SLC19A1	-1.62
ILMN_2464999	SLC25A38	-1.66
ILMN_2721919	SLC30A6	-1.91
ILMN_2454880	SLC35A1	-1.75
ILMN_2755424	SLC35B3	-2.62
ILMN_2741872	SLC39A13	-2.58
ILMN_2681776	SLC39A6	-3.07
ILMN_2760977	SLC7A7	-1.90
ILMN_1218325	SMC1A	-1.68
ILMN_3064134	SNAP91	-2.80
ILMN_2760540	SNIP1	-1.87
ILMN_2616000	SNTB2	-2.86
ILMN_2515349	SNX2	-1.56
ILMN_2712305	SPATA6	-1.61
ILMN_2835723	SPG20	-2.11
ILMN_2732689	SPOCK3	-2.09
ILMN_2435505	SPSB1	-2.10
ILMN_2953277	SQLE	-1.88
ILMN_2424299	SRA1	-1.54
ILMN_2965093	SRPK2	-1.59
ILMN_1216663	ST6GALNAC5	-1.78
ILMN_1233531	STARD3NL	-2.09
ILMN_2850839	STAT2	-1.56
ILMN_2633148	STXBP1	-2.68
ILMN_2645662	SURF1	-1.91
ILMN_2759983	SUV39H1	-2.04
ILMN_3136196	TAF6	-1.95
ILMN_2658266	TALDO1	-1.95
ILMN_1225390	TANK	-1.85
ILMN_2974720	TBC1D9	-1.64
ILMN_2696299	TEX10	-1.72
ILMN_2819679	THAP11	-2.12
ILMN_2602597	THNSL1	-1.90
ILMN_2706857	THNSL2	-1.54
ILMN_2952841	THOC1	-2.01
ILMN_1227602	TK2	-1.56
ILMN_2668289	TMEM127	-1.96
ILMN_2460043	TMEM130	-1.78
ILMN_1238680	TMEM176A	-1.61
ILMN_2476885	TMEM184C	-2.00
ILMN_2724409	TMEM5	-2.81
ILMN_2461800	TMEM50A	-1.66
ILMN_2724235	TMEM59L	-1.65
ILMN_2646241	TMEM86A	-1.88
ILMN_2847136	TNFRSF12A	-1.62
ILMN_3011719	TRAF7	-1.61
ILMN_2460745	TRIB2	-2.43
ILMN_2836924	TRMT1	-1.78
ILMN_1236303	TSPAN6	-3.19
ILMN_2828302	TSSC1	-2.13
ILMN_2698911	TSSC4	-4.72
ILMN_1212648	TTC13	-1.91
ILMN_2698757	TXNL4	-1.55
ILMN_1243908	UBAP2	-1.65
ILMN_2901227	UBE2G1	-3.18
ILMN_2750035	UHRF1BP1L	-1.77
ILMN_2987161	ULK1	-2.97
ILMN_2935796	UNC119	-1.66
ILMN_1254630	UROD	-1.79
ILMN_2702787	USE1	-1.85
ILMN_2955322	USF1	-1.81
ILMN_2724194	USP47	-1.80
ILMN_1225544	VKORC1L1	-3.04
ILMN_2739517	VLDLR	-2.07
ILMN_2746968	WDR1	-1.83
ILMN_2685903	WDR21	-2.36
ILMN_1219459	WDR45	-1.68
ILMN_1228320	WDR68	-2.05
ILMN_1253692	WDSOF1	-1.76
ILMN_2655907	XIST	-2.10
ILMN_3079138	XPNPEP3	-2.01
ILMN_1231457	YEATS4	-1.68
ILMN_2993720	YIF1A	-2.22
ILMN_2998135	ZC3H18	-1.53
ILMN_2753149	ZCCHC8	-2.46
ILMN_2755243	ZEB2	-1.79
ILMN_3003518	ZER1	-1.59
ILMN_1213456	ZFP160	-3.21
ILMN_2729953	ZFP397	-2.13
ILMN_2912439	ZFP41	-1.98
ILMN_3002284	ZFP410	-3.83
ILMN_2866099	ZFP579	-1.69
ILMN_2850527	ZFP64	-1.64
ILMN_1228165	ZFP644	-1.77
ILMN_1244819	ZFP661	-1.55
ILMN_2982890	ZFP692	-2.80
ILMN_1244619	ZFP768	-2.12
ILMN_1233545	ZFP787	-1.80
ILMN_2711892	ZHX3	-2.03
ILMN_3142097	ZMPSTE24	-2.40
ILMN_1237571	ZMYND11	-2.07

Cho et al., Table S4 (related to figure 2B)

Supplemental Tables

Table S1. mRNA expression fold changes of genes known as HIF-1α target genes after axotomy *in vitro*. (Related to figure 1A).

HIF-1α-target genes from the reference (Benita et al., 2009) were selected from the microarray results previously performed (Cho et al., 2013) and listed with expression fold changes at different hours after axotomy. PID indicates the Pubmed ID for the individual reference showing the evidence of HIF-1α-dependency. The 3h, 8h, 12h and 40h indicate the time after *in vitro* axotomy. Each value indicates $\log_2$-transformed expression fold changes. The red dot indicates the highest up-regulation at the indicated hours after axotomy over 0.263. The gray dot indicates the mild up-regulation at the indicated hours after axotomy over 0 and below 0.263. The black dot indicates the down-regulation at the indicated hours after axotomy

Table S2. mRNA expression fold changes of genes predicted as HIF-1 target genes after axotomy *in vitro*. (Related to figure 1B).

Predicted HIF-1α-target genes from the reference (Ortiz-Barahona et al., 2010) were selected from the microarray result previously performed (Cho et al., 2013) and listed with expression fold changes at different hours after axotomy. The 3h, 8h, 12h and 40h indicate the time after *in vitro* axotomy. Each value indicates $\log_2$-transformed expression fold changes. The red dot indicates the highest up-regulation at the indicated hours after axotomy over 0.263. The gray dot indicates the mild up-regulation at the indicated hours after axotomy over 0 and below 0.263. The black dot indicates the down-regulation at the indicated hours after axotomy

Table S3. List of genes up-regulated by constitutive overexpression of HIF-1α. (Related

to figure 2B).

Probe indicates Illumina gene ID. The number indicates log_2-transformed average fold change by constitutive overexpression of HIF-1α (green, log2[average fold]=<1.20; orange, 1.20< log2[average fold]<1.9; red, 1.9=<log2[average fold]).

Table S4. List of genes down-regulated by constitutive overexpression of HIF-1α. (Related to figure 2B).

Probe indicates Illumina gene ID. The number indicates log_2-transformed average fold change by constitutive overexpression of HIF-1α (gray, -2.0=<log2[average fold]; light blue, -2.0< log2[average fold]<-2.9; blue, log2[average fold]=<-2.9).

Table S5. List of genes screened as HIF-1α-dependent injury-induced genes (1 to 493) (Related to figure 2C).

Probe indicates Illumina gene ID. The number "Cslope" or "KSlope" indicates the calculated slopes of relative fold changes of expression. The number "O/C" indicates the relative expression level of genes in HIF-1α-overexpressing DRG neurons over control DRG neurons (see Experimental Procedures for details; RNA preparations, qPCR and microarray analyses).

Supplemental Experimental Procedures

Antibodies and lentiviruses

The following antibodies were used in this study: anti-HIF-1α (Novus, NB100-479; Abcam, ab113642 and ab2185), anti-SCG10 (Novus, NBP1-49461), anti-βIII tubulin (Covance, MMS-435P), anti-GFP (Santa Cruz, sc-9996), anti-p-PKCμ (Cell Signaling, #2051), anti-PKCμ (Cell Signaling, #2052), anti-PKCδ (Cell Signaling, #9616), anti-p-PKC (pan) (Cell Signaling, #9371), anti-p-JNK (Cell Signaling, #9912), anti-p-c-Jun (Cell Signaling, #9261), anti-c-Jun (Cell Signaling, #9165) and anti-DLK (Antibodies Incorporated, #75-355). To express HIF-1α in cultured DRG neurons, human HIF1A cDNA (Addgene, 18949) was sub-cloned into FUGW lentiviral vector for constitutively overexpression. HA-HIF1alpha-pcDNA3 was a gift from Dr. William Kaelin (Addgene plasmid #18949 (Kondo et al., 2002). For inducible expression, human HIF1A cDNA was sub-cloned into tetracycline-responsive lentiviral expression vector LV-TRE-GFP-Ubi-rtTA3 by the Viral Vector Core (Washington University, School of Medicine). Mouse VEGF 164 (493-MV-025/CF) from R&D systems was used in sciatic nerve regeneration assays.

Lentiviral-mediated knock down of HIF-1α and selected HIF-1α dependent genes.

To knock down HIF-1α and selected HIF-1α dependent genes for *in vitro* regeneration assay, MISSION shRNAs from Sigma were used and lentiviruses were generated as previously described (Cho and Cavalli, 2012). MISSION shRNAs from Sigma were used: HIF-1α, TRCN0000232222, TRCN0000232223; PDE1B, TRCN0000438413, TRCN0000434573; HMOX1, TRCN0000234077, TRCN0000234075; MAP3K1, TRCN0000361582, TRCN0000361513; ARHGEF3, TRCN0000110045, TRCN0000110048; ARHGAP29, TRCN0000023924, TRCN0000023926; NGFR, TRCN0000065555, TRCN0000065554; VEGFA, TRCN0000066818, TRCN0000066822, TRCN0000315978).

Meta analysis and Microarray analyses

Raw data from our previous microarray (Cho et al., 2013) was used to obtain a list of genes up- regulated at 0, 3, 8, 12 and 40 h after *in vitro* axotomy. Quantile normalized expression levels were used. Genes with *p* value less than 0.01 at each time-point and with a fold expression change at any point >1.2 compared to the 0 h control were included in our list of injury-induced genes. This list of injury-induced genes was compared with lists of known HIF-1α-known target genes (Benita et al., 2009) or HIF-1α-predicted target genes (Ortiz-Barahona et al., 2010).

To study HIF-1α-dependent gene regulation, a microarray analysis was done as previously described (Cho et al., 2013), comparing control DRG neurons to DRG neurons in which HIF1A was knocked down or DRG neurons in which human HIF1A was overexpressed. Total RNA was extracted at 0, 3 and 12 h after axotomy from control cultured DRG neurons, DRG neurons in which, HIF1A was knocked down or DRG neurons in which human HIF1A was overexpressed. To analyze expression profile, MouseRef-8 v2.0 Bead-Chips (Illumina) from Genome Technology Access Center at Washington University was used. To screen for the minimal sets of injury-responsive HIF-1α-dependent genes, the genes detected with *p* value smaller than 0.1 were selected. Injury-responsive genes were then filtered by expression level at 3 or 12 hours after axotomy. Only genes with expression levels 16% higher at 3 or 12 hours than at 0 hour time point were selected ([expression level_3 hours] / [expression level_0 hour] > 1.16 OR [expression level_12 hours] / [expression level_0 hour] > 1.16). To screen for HIF-1α-dependent genes, "slope of expression level" was calculated. The slope of expression level was calculated using the gene expression fold change at 0, 3 and 12 hours after axotomy from the control sets ("Cslope") or HIF-1α-knock down sets ("Kslope"). Based on the calculated slope, only the genes that have a higher slope in the control sets compared to HIF-1α-knock down sets either at 3 or 12 hours were selected. ([expression level of control_3 hours] / [expression level of

HIF-1α-knock down_3 hours] > 1 OR [expression level of control_12 hours] / [expression level of HIF-1α-knock down_12 hours] > 1). To further restrict the HIF-1α-dependency, only the genes showing higher expression level in overexpressed HIF-1α compared to the control were selected ([expression level of HIF-1α-overexpression_0 > [expression level of control_0 hour], O/C).

Surgeries and tissue preparations

Sciatic nerve injury experiments were performed as described (Cho and Cavalli, 2012). For double crush injury experiments, we followed previous protocols (Shin et al., 2012). Birefly, the nerve was crushed with fine forceps for 20 s. The site of the first injury was marked by dipping the tips of forceps in 1μm orange fluorescence beads (FluoSpheres; Invitrogen). The second crush was given at 1mm proximal to the first crush site under an SZX12 fluorescence-dissecting microscope (Olympus) to injure all axons.

For mouse L4 dorsal root nerve crush surgery, an ~2cm skin incision was made above the L2 vertebra and the soft tissue below dissected. Mice were then placed in a custom frame with 2 horizontal stainless steel ‘arms’ that were slid under each L2 transverse process in order to stabilize the mouse. The connective tissue between the L2 and L3 vertebra was then removed and a small laminectomy of the caudal portion of the L2 vertebra was performed to create a small opening exposing the spinal cord and lumbar dorsal roots. Fine forceps were then used to pierce through the dura perpendicular to the spinal cord and crush the right L4 dorsal root ~6mm from the L4 DRG for 5 seconds. The underlying tissue was sutured with 6.0 silk sutures and the skin closed with metal clips.

For western blot analysis, mouse DRG tissues were dissected at the indicated time after nerve injury. Mouse DRG tissues were homogenized in lysis buffer (Cell Signaling) as described (Cho and Cavalli, 2012). Protein concentration was quantified by Bio-Rad protein assay kit (Bio-

Rad). For immunohistochemistry, mouse DRG tissues were prepared as described (Cho and Cavalli, 2012). L4 or L5 DRG were dissected and fixed for 1 hour in 4% paraformaldehyde in PBS, incubated overnight in 30% sucrose, embedded in OCT solution (Tissue-Tek) and frozen in dry ice-cooled methylbutane. 10μm cryostat sections were stained with the indicated antibodies using standard methods. To measure the intensity of nuclear HIF-1α, region-of-interest (ROI) of DAPI-positive area from TUJ-1-positive cells was selected and HIF-1α-fluorescence intensity was measured using ImageJ.

Embryonic DRG neuron spot culture and *in vitro* regeneration assay

Embryonic DRG neurons were cultured as previously described (Cho and Cavalli, 2012). Briefly, DRG neurons of mouse embryos at E13.5 were dissected, and trypsinized and dissociated. For spot culture, 10,000 DRG neurons were resuspended in 2.5 µl of medium and plated on PDL/laminin-coated culture dishes and incubated for 20 minutes before adding more medium. To knock down or overexpressing HIF-1α, or knock down HIF-1α target genes, lentiviruses were infected at DIV4. *In vitro* regeneration assay was performed as previously described (Cho and Cavalli, 2012). DRG spot cultures were axotomized with a blade (FST, 10035-10) at DIV7 under a dissection scope (Nikon, SMZ645) and immunostained for SCG10 and βIII tubulin antibodies. Images were acquired on a Nikon, TE2000E microscope. A regeneration index was calculated from the images acquired 40 h post axotomy by measuring the fluorescence intensity of a square area (2.7x0.1mm) at 0.1 mm distal to the axotomy line and normalizing this intensity to the similar area 0.1 mm proximal to the axotomy line.

***In vivo* regeneration assays**

To test for axon regeneration *in vivo,* sciatic nerves were dissected at the indicated time after a crush injury. Longitudinal sections of fixed sciatic nerves were stained with SCG10 and TUJ1, as described in (Shin et al., 2012). For each animal, SCG10 fluorescence intensity was measured along the length of the nerve using a line scan macro in ImageJ in five serial sections. A regeneration index was calculated by measuring the average SCG10 intensity at several distances away from the crush site, which is defined by the position along the sciatic nerve length with maximal SCG10 intensity (Shin et al., 2014). To measure reinnervation of the neuromuscular junction after sciatic nerve injury, the tibialis anterior muscle as well as the distal 5 mm of the deep peroneal nerve from thy1-YFP16 mice was removed and the extensor hallucis longus (EHL) muscle was dissected, fixed and stained with Alexa Fluor 647-conjugated α-bungarotoxin (Invitrogen) and mounted for confocal imaging. The number of NMJ endplates re-occupied (O) or non-occupied (N) by YFP signal was counted and normalized to the total number of endplates to calculate the percentage.

Hypoxia treatment

For *in vitro* hypoxia, established protocols were followed (Wu and Yotnda, 2011). Briefly, embryonic DRG cultures were placed in a gas-tight hypoxia chamber containing a Petri dish filled with sterile water to maintain humidity. To obtain hypoxic condition, a tube attached to a gas tank containing 5% CO_2 balanced with nitrogen was connected to the chamber with airtight connector. The air in the chamber was flushed for 10 minutes by opening the gas tank at a flow rate of 20 L/min. The chamber was then placed back in the cell culture incubator for the indicated amount of time. Control cultures underwent the same procedure but the air in the control chamber was flushed with 5% CO_2 balanced with normal air.

For *in vivo* hypoxia, all procedures were approved by Washington University in St. Louis, School of Medicine Animal Studies Committee. To perform whole body-hypoxia treatment, an established protocol (Zhang et al., 2004) was followed with minor modifications. Briefly, conscious mice were exposed to AIH by being placed in a gas-tight chamber (E-Z Anesthesia).

Air was continuously flushed at a rate of 1L/min. Chamber was flushed with oxygen balanced with nitrogen: 10 min episodes of 8% O_2; 10 min intervals with normal air. After 6 hypoxic episodes with equivalent normoxic intervals (120min) the mice were returned to their cages until the next exposure. For sciatic nerve axon regeneration experiments, the 120 min AIH protocol began 2 hours after sciatic nerve injury and was applied once daily for 3 days. For muscle reinnervation experiments, the 120 min AIH protocol was administered daily for 7 days starting 1 hour after sciatic nerve injury and mice were returned to their cages for 5 days. For control groups, mice were placed in the chamber for the same durations but normal air was supplied.